Modeling Elastically Mediated Liquid-Liquid Phase Separation

Xuefeng Wei,[1,2,*] Jiajia Zhou,[3,4,*] Yanting Wang,[1,2] and Fanlong Meng[1,2,†]
[1]*CAS Key Laboratory of Theoretical Physics, Institute of Theoretical Physics, Chinese Academy of Sciences, Beijing 100190, China*
[2]*School of Physical Sciences, University of Chinese Academy of Sciences, 19A Yuquan Road, Beijing 100049, China*
[3]*Key Laboratory of Bio-Inspired Smart Interfacial Science and Technology of Ministry of Education,*
School of Chemistry, Beihang University, Beijing 100191, China
[4]*Center of Soft Matter Physics and Its Applications, Beihang University, Beijing 100191, China*

(Received 19 August 2020; accepted 16 November 2020; published 22 December 2020)

We propose a continuum theory of the liquid-liquid phase separation in an elastic network, where phase-separated microscopic droplets rich in one fluid component can form as an interplay of fluids mixing, droplet nucleation, network deformation, thermodynamic fluctuation, etc. We find that the size of the phase-separated droplets decreases with the shear modulus of the elastic network in the form of $\propto [\text{modulus}]^{-1/3}$ and the number density of the droplet increases almost linearly with the shear modulus $\propto [\text{modulus}]$, which are verified by the experimental observations. Phase diagrams in the space of (fluid constitution, mixture interaction, network modulus) are provided, which can help to understand similar phase separations in biological cells and also to guide fabrications of synthetic cells with desired phase properties.

DOI: 10.1103/PhysRevLett.125.268001

Membraneless compartments (organelles) in cells are often supramolecular assemblies composed of proteins, nucleic acids, and other molecules [1–4]. Examples include nucleolus in the nucleus, stress granules, centrosomes in the cytoplasm, etc., and they usually provide physical constraints for specific biochemical reactions. After the liquidlike features of some membraneless compartments, represented by *P* granules [5] and *Xenopus* germinal vesicles [6], were experimentally identified, liquid-liquid phase separation was proposed as a plausible mechanism for the formation of such membraneless compartments [7–11]. Different from typical liquid-liquid phase separation in a one component system [12–14] or multicomponent mixtures [15,16], where the mixing energy of liquids is deterministic of whether phase separation can occur or not, the case in cells is usually more complicated due to the elastic constraint by the cytoskeleton [17,18]. Thus, exploring the role of the elastic network in liquid-liquid phase separation will be important in understanding and predicting the properties of the phase-separated products.

Attempting to learn how an elastic network can influence the phase-separated products of liquid-liquid phase separation, there are recent experimental studies [19,20] investigating the liquid-liquid phase separation of a fluorinated oil-silicone oil mixture in a silicone polymer network. It is found that the liquid-liquid phase separation can occur with the formation of droplets rich in one fluid component (fluorinated oil); with the increase of the elastic modulus of the network, the droplet size decreases, while the number density of the droplets increases (see Fig. 1). The critical concentration of the fluorinated oil for its condensation (droplet formation) in the elastic network has been related with the stiffness of the network by thermodynamic arguments [21,22] and the dynamics of droplets due to stiffness gradient is discussed [23,24], while how to theoretically characterize the relation between the droplet properties (size, number density, etc.) and the network elasticity remains unclear. The main difficulty lies in how to deal with the system complexity incorporating mixing of different fluids, droplet nucleation in a polymer network, thermodynamic fluctuation, etc.

In this Letter, we treat the liquid-liquid phase separation of an A/B fluid mixture in an elastic polymer network.

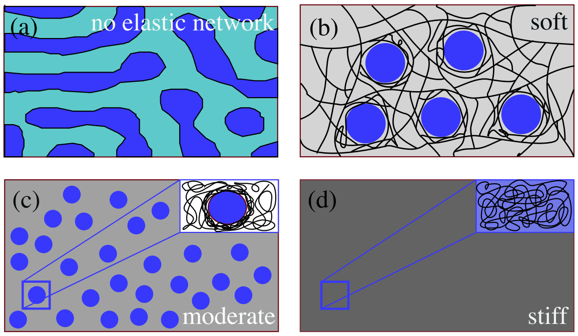

FIG. 1. (a) Liquid-liquid phase separation in a free space (without elastic network). (b) A few large droplets form in a soft elastic network (small shear modulus). (c) Many small droplets form in a moderate elastic network (moderate shear modulus). (d) Inhibition of phase separation in a stiff elastic network (large shear modulus).

By constructing a free energy model of the system, which incorporates the mixing entropy, the Flory-Huggins-type interaction among the fluid mixture, the surface energy of phase-separated droplets, and the elastic energy of the droplets-deforming polymer network, we discuss thoroughly how network elasticity determines the conditions of the phase separation and the properties of phase-separated products, where the results are also compared with the experiments.

When the liquid-liquid phase separation occurs, droplets rich in one fluid component will form, and the number density and the radius of the droplets are denoted as n and R, respectively; then the volume fraction of the droplets is equal to $\nu = 4\pi n R^3/3$. Here we assume that the droplets are monodisperse in size, following the experimental observations [19], and such monodispersity mainly results from the elastic constraint by the polymer network. Considering the volume conservation of the A component, there is the relation between the volume fraction of the A component in the droplets ϕ_A^d and that in the bulk ϕ_A^b as

$$\nu\phi_A^d + (1-\nu)\phi_A^b = \phi_A^0, \tag{1}$$

where ϕ_A^0 is the volume fraction of the A component in the prepared state (before phase separation). The free energy density of the system can be expressed as

$$\begin{aligned}\mathcal{F}(\phi_A^d, \phi_A^b, \nu, R) = {}& \nu f_{\text{mix}}(\phi_A^d) + (1-\nu) f_{\text{mix}}(\phi_A^b) \\ & + 3\nu\frac{\gamma}{R} + \nu f_{\text{el}}(R) \\ & - \xi[\nu\phi_A^d + (1-\nu)\phi_A^b - \phi_A^0].\end{aligned} \tag{2}$$

The first and the second term on the right-hand side of Eq. (2) denote the mixing free energy density of two fluids (without elastic constraint) inside and outside of the droplets, respectively. For this free energy density $f_{\text{mix}}(\phi_A)$, we adopt the typical Flory-Huggins form [25], which consists of the mixing entropy and the interaction between the fluids: $f_{\text{mix}}(\phi_A) = (k_{\text{B}}T/v_A)[\phi_A \ln\phi_A + (v_A/v_B)\phi_B \ln\phi_B + \chi\phi_A\phi_B]$, where k_{B} is the Boltzmann constant, T is the temperature, v_A and v_B denote the volume of one A and one B liquid molecule, respectively, $\phi_B = 1 - \phi_A$ is the volume fraction of the B component and χ is the Flory-Huggins parameter characterizing the interaction between A and B liquids. Note that we treat the network component the same as the B component in order to compare with relevant experiments in the later discussion, while it is straightforward to adapt the theory to the case where the network component is different from the A or B component. The third term in Eq. (2) denotes the interfacial energy density of the droplets where γ is the surface tension. The fourth term in Eq. (2) denotes the elastic energy induced by the droplets deforming the incompressible elastic network [26,27]. The explicit expression of f_{el} is taken as $f_{\text{el}}(R) = 3[1-(R_0/R)^3]\int_1^{R/R_0} \lambda^2 W(\lambda)/(\lambda^3-1)^2 d\lambda$ (see Ref. [26] or Supplemental Material [28] for details), where $R_0 \simeq (k_{\text{B}}T/G)^{1/3}$ [29] denotes the mesh size of the network with G as the shear modulus of the elastic network, e.g., $R_0 \simeq 0.01$ μm for $G \simeq 5$ kPa. The function $W(\lambda)$ in this elastic term represents the elastic energy density of an inflated spherical shell (like a thin spherical balloon), for which we take the Gent model [30,31], i.e., $W(\lambda) = -\frac{1}{2}GJ_m \ln[1 - J(\lambda)/J_m]$, where $J(\lambda) = 2\lambda^2 + \lambda^{-4} - 3$ with λ as the stretch ratio in the radial direction, and J_m is a phenomenological parameter characterizing the finite stretchability of the material (it is a fitting parameter in later comparisons with experiments). Note that, if the deformation is small, i.e., $\lambda \to 1$, the Gent model reduces to the neo-Hookean model, with $W(\lambda) = \frac{1}{2}GJ(\lambda)$. The last term in Eq. (2) comes from the constraint in Eq. (1) with ξ as a Lagrangian multiplier.

Chemical and mechanical balance.—By optimizing the total energy density with respect to the volume fraction of the A component in the phase-separated droplets ϕ_A^d and that in the bulk ϕ_A^b, respectively, $\partial\mathcal{F}/\partial\phi_A^d = \partial\mathcal{F}/\partial\phi_A^b = 0$, one can easily identify ξ as the chemical potential,

$$\xi = f'_{\text{mix}}(\phi_A^d) = f'_{\text{mix}}(\phi_A^b). \tag{3}$$

In other words, the chemical potential of the A (B) component in the phase-separated droplets and in the bulk should be equal. By optimizing the energy density with respect to the volume fraction ν, i.e., $\partial\mathcal{F}/\partial\nu = 0$, there is the relation $f_{\text{mix}}(\phi_A^d) - f_{\text{mix}}(\phi_A^b) - \xi(\phi_A^d - \phi_A^b) + 3\gamma/R + f_{\text{el}}(R) = 0$. With the substitution of the chemical potential $\xi = f'_{\text{mix}}(\phi_A^d) = f'_{\text{mix}}(\phi_A^b)$, the pressure difference between the droplet and the bulk ΔP should obey

$$\Delta P = \Pi(\phi_A^d) - \Pi(\phi_A^b) = \frac{3\gamma}{R} + f_{\text{el}}(R), \tag{4}$$

where $\Pi(\phi_A^d)$ and $\Pi(\phi_A^b)$ denote the osmotic pressure in the droplet and in the bulk, respectively, by recalling $\Pi(\phi_A) = -f_{\text{mix}}(\phi_A) + \phi_A f'_{\text{mix}}(\phi_A)$. Equation (4) indicates the mechanical balance between the osmotic pressure, the surface tension, and the elastic pressure. The inclusion of the elastic contribution might induce different growth of the droplets than the standard Ostwald ripening [20].

Droplet size and density.—Droplets rich in either A or B component will form when liquid-liquid phase separation occurs. After assuming that the droplets are monodisperse, the size of droplets can be obtained by optimizing the total energy density with respect to the radius of phase-separated droplets R, $\partial\mathcal{F}/\partial R = -3\nu\gamma/R^2 + \nu df_{\text{el}}/dR = 0$, obtaining

$$\frac{3\gamma}{R^2} = \frac{df_{\text{el}}}{dR}. \tag{5}$$

Equation (5) indicates that the size of the droplets is determined by the competition between the surface tension of the droplets and the elastic contribution of the deformed elastic medium. By introducing the ratio between the droplet radius and the mesh size of the network, $\lambda_R = R/R_0$, we can rewrite Eq. (5) as $3\alpha_\mathrm{T} = \lambda_R^2/G \times df_\mathrm{el}/d\lambda|_{\lambda=\lambda_R}$ with the "thermal elastocapillary number" defined as $\alpha_\mathrm{T} = \gamma/(GR_0) = \gamma/[G^{2/3}(k_\mathrm{B}T)^{1/3}]$, where the mesh size is $R_0 \simeq (k_\mathrm{B}T/G)^{1/3}$. Alternatively, we can define a function $g(\lambda_R)$

$$g(\lambda_R) = \frac{\lambda_R^2}{G}\frac{df_\mathrm{el}}{d\lambda}\bigg|_{\lambda=\lambda_R} \simeq \frac{3\lambda_R^4}{G(\lambda_R^3-1)^2}W(\lambda_R), \qquad \lambda_R \gg 1, \qquad (6)$$

for which one can refer to the Supplemental Material [28] for more details. Once we know the thermal elastocapillary number α_T (given by the surface tension and the shear modulus), then the droplet radius can be obtained as $\lambda_R = g^{-1}(3\alpha_\mathrm{T})$, $R = R_0 g^{-1}(3\alpha_\mathrm{T})$.

With the Gent model, the ratio of the droplet radius to the mesh size of the network λ_R increases with α_T and soon approaches its limiting value λ_m where $\lambda_m \to \sqrt{J_m/2}$ for $J_m \gg 1$. In the range of $\alpha_\mathrm{T} > 5$, the approximated solution is

$$\lambda_R \simeq \lambda_m, \qquad R \simeq \lambda_m R_0, \qquad (7)$$

meaning that the size of the droplet is essentially determined by the limiting stretchability and the mesh size of the material if α_T is sufficiently large. One can show that the implementation of the finite stretchability in the Gent model is very important in predicting the droplet size, while elastic models without this implementation, e.g., the neo-Hookean model, does not work (see Supplemental Material [28]). For the Gent model with $\lambda_m > 100$, the pressure difference between the droplet and the bulk, ΔP in Eq. (4), is almost a constant: $\Delta P \simeq 5G/2$ [32,33]. Apart from such elastically mediated liquid-liquid phase separation, there can be other possible means to form the finite-sized membraneless organelles, e.g., by balancing the short-range attraction (van der Waals interaction, etc.) and the long-range repulsion (Coulomb interaction, etc.) among fluid components [34,35] and by limiting the molecule supply for building the phase-separated organelles [9,36].

Comparison with experiment.—In the experiments [19], a fluorinated oil-silicone oil mixture is first prepared in a silicone polymer network at 45 °C, with the fluorinated oil at its saturation volume fraction, i.e., $\phi_\mathrm{sat}(45\,^\circ\mathrm{C}) \simeq 0.038$. (saturation volume fraction ϕ_sat: critical volume fraction where a free binary fluid mixture without elastic network starts phase separation). Then by quenching the system to 23 °C, at which a free mixture would have a lower saturation volume fraction [$\phi_\mathrm{sat}(23\,^\circ\mathrm{C}) \simeq 0.028$], phase separation takes place with the formation of microsized droplets rich in the fluorinated oil. By taking the A and B components in the model as the fluorinated oil and the silicone oil, respectively, we can directly compare the theoretical results with the experiments. In the experiments [19], $v_A \simeq 3.7 \times 10^{-28}$ and $v_B \simeq 4.8 \times 10^{-26}\ \mathrm{m}^3$. The surface tension is $\gamma \simeq 0.004\ \mathrm{N/m}$ and the Flory-Huggins parameter at 23 °C is $\chi = 2.763$. In this particular experiment, although surface tension is important in determining the size of phase-separated droplets as shown in Eq. (5), its contribution is negligible in the criterion of phase separation compared with other terms (osmotic pressure and elastic contribution) in Eq. (4) after assuming the spherical shape of the droplets.

As shown in Fig. 2(a), the droplet size decreases with the shear modulus of the elastic network, matching with the experimental observations, and there is a relation between the droplet size and shear modulus: $R \simeq (k_\mathrm{B}T)^{1/3}(J_m/2)^{1/2}G^{-1/3}$, following the analytic expression in Eq. (7). Note that the stretching limit

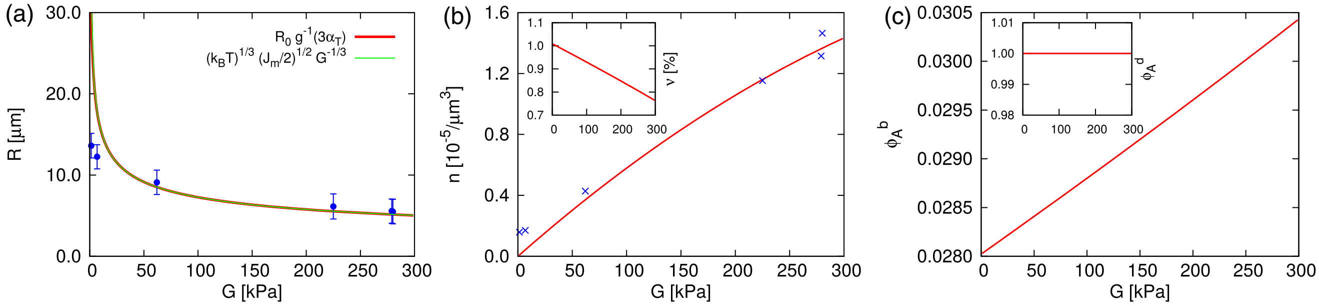

FIG. 2. (a) Droplet radius, (b) number density, and (c) volume fraction of fluorinated oil (A component) in the bulk ϕ_A^b as a function of the shear modulus of the elastic network. (b),(c) Inset: denotes the volume fraction of phase-separated droplets ν and the volume fraction of fluorinated oil (A component) in the droplets ϕ_A^d as a function of the shear modulus of the elastic network, respectively. The red line in (a) is obtained by $R = R_0 g^{-1}(3\alpha_\mathrm{T})$ and the green line in (a) is obtained by $R \simeq (k_\mathrm{B}T)^{1/3}(J_m/2)^{1/2}G^{-1/3}$. The red lines in (b) and (c) are obtained by minimizing the energy in Eq. (2). The blue dots in (a) and (b) are experimental data [19]. Parameters are taken as follows: volume fraction of fluorinated oil at the prepared state (before phase separation) $\phi_A^0 = 0.038$ (saturation volume fraction ϕ_sat at 45 °C, volume of one fluorinated oil molecule $v_A = 3.7 \times 10^{-28}\ \mathrm{m}^3$, volume of one silicone oil molecule $v_B = 4.8 \times 10^{-26}\ \mathrm{m}^3$, surface tension $\gamma = 0.004\ \mathrm{N/m}$, the Flory-Huggins parameter $\chi = 2.763$, and $J_m = 8.82 \times 10^6$ in the Gent model.

$J_m = 8.82 \times 10^6$ is taken as a constant, which is independent of the shear modulus. One can also introduce the dependence of J_m on the shear modulus (see Supplemental Material [28]) and can easily obtain a better fitting in Fig. 2(a), but here we will keep J_m as a constant for simplicity. In experimental measurements, Young's modulus was used for describing the network elasticity $E = 3G$, and this conversion is taken into account in the comparison between the theory and the experiments. As noted in the inset of Fig. 2(b), the volume fraction of droplets ν slightly decreases by increasing the shear modulus, in the form of $\nu = -8 \times 10^{-6}\ \mathrm{kPa}^{-1} \times G + 0.01$ (changing from $\nu \simeq 1\%$ without elastic network to $\nu \simeq 0.76\%$ in a stiff network with $G = 300$ kPa). Meanwhile, the number density of the droplets can be obtained as $n = 3\nu/(4\pi R^3) \simeq 6\sqrt{2}\nu G/(4\pi k_\mathrm{B} T J_m^{3/2})$, which basically increases linearly with the shear modulus, $n \propto G$ for small G as shown in Fig. 2(b). In other words, more and smaller droplets will form if the elastic network is stiffer. Remarkably, when phase separation occurs, the volume fraction of fluorinated oil (A component) in the droplets ϕ_A^d remains almost as a constant ($1 - \phi_A^d \sim 10^{-102}$) regardless of the shear modulus G as shown in the inset of Fig. 2(c), while its volume fraction in the bulk increases almost linearly with the shear modulus, $\phi_A^b(G) \simeq \phi_A^b(0) - \nu = 0.028 + 8 \times 10^{-6}\ \mathrm{kPa}^{-1} \times G$ as shown in Fig. 2(c); this means that the droplets consist of almost pure fluorinated oil.

In experiments, the shear modulus of the elastic network is taken as a controllable parameter, where such an elastic constraint can control the size of phase-separated droplets as discussed above. Meanwhile, the elastic constraint can also inhibit the liquid-liquid phase separation. Figure 3(a) shows the phase diagram in the $\phi_A - \chi$ plane for different shear modulus G. At small χ, the system is homogeneous. When the network is absent, the system is a binary mixture of A/B with an aspect ratio $N = v_B/v_A$. There is a critical point at $(\phi_A)_c = 1/(\sqrt{N}+1), \chi_c = 1/2 + 1/\sqrt{N} + 1/(2N)$ [37]. When $\chi > \chi_c$, there is a certain regime of ϕ_A at which the homogeneous state becomes unstable and phase separation proceeds. The presence of the elastic network moves the binodal line upward in the small-ϕ_A region. Therefore, there are regions between the colored lines and the black line in Fig. 3(a) where the homogeneous phase remains stable in presence of the elastic network. The critical value of the Flory-Huggins parameter χ_c increases with the increasing shear modulus G. This is more clear in Fig. 3(b), which shows the phase diagram in the ϕ_A–G plane for different values of χ. At small G, there is a range of ϕ_A where the homogeneous state is unstable. The unstable region will be slightly reduced by increasing the shear modulus, and when the critical value of G_c is reached, the phase-separated region disappears and the homogeneous state becomes stable.

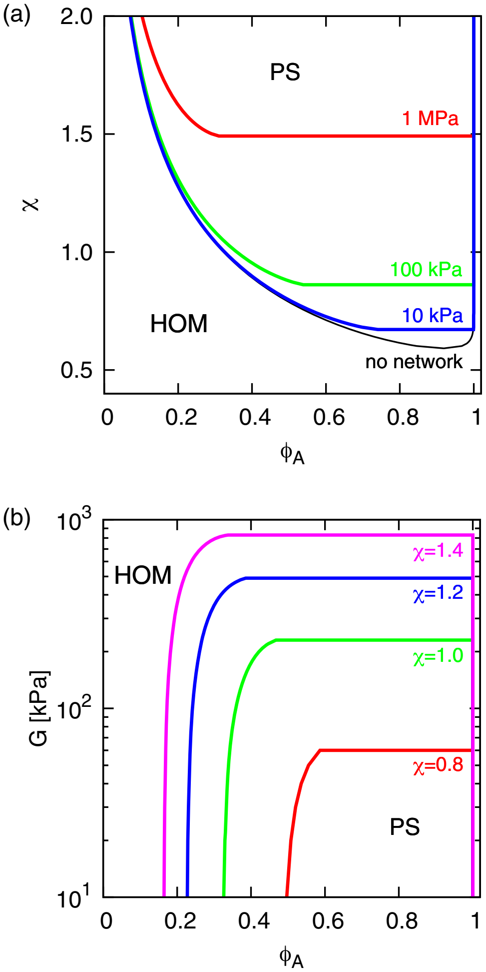

FIG. 3. Phase diagram of elastically mediated liquid-liquid phase separation (a) in the plane of (ϕ_A, χ) for different shear modulus G and (b) in the plane of (ϕ_A, G) for different Flory-Huggins parameter χ. HOM, homogeneous state without phase separation; PS, phase separation. Parameters are taken as follows: volume of one fluorinated oil molecule $v_A = 3.7 \times 10^{-28}$ m^3, and volume of one silicone oil molecule $v_B = 4.8 \times 10^{-26}$ m^3.

In conclusion, we propose a continuum model of liquid-liquid phase separation in an elastic network incorporating fluids mixing, droplet nucleation, network deformation, thermodynamic fluctuation, etc., and investigate quantitatively how network elasticity can influence such phenomenon. When the phase separation occurs, the size of the phase-separated droplets is found to decrease with the increasing network elasticity in the form of a scaling law, and the number density of the droplets increases almost linearly; the theoretical results are verified by experimental observations. Furthermore, phase diagrams in the planes of Flory-Huggins parameter, shear modulus, and the volume fraction of liquid compositions are constructed, providing necessary conditions for liquid-liquid phase separation in an elastic medium. This portable model can be easily generalized to deal with the elastically mediated liquid-liquid phase transition in more complicated systems such as an elastically constrained ternary, quaternary,…, fluid mixture, and can be predictive for producing phase-separated droplets of desired size and density. Moreover, we hope it can also provide new insight into the formation of membraneless organelles constrained by cytoskeleton.

This work is supported by the Strategic Priority Research Program of Chinese Academy of Sciences (Grant No. XDA17010504) and the National Natural Science Foundation of China (Grants No. 11947302 and No. 21774004). F. M. acknowledges partial funding from Alexander von Humboldt Foundation. The computations of this work were conducted on the HPC cluster of ITP-CAS.

---

[*] These authors contributed equally to this work.

[†] Corresponding author.
fanlong.meng@itp.ac.cn

[1] H. B. Schmidt and D. Görlich, Trends Biochem. Sci. **41**, 46 (2016).

[2] V. N. Uversky, Curr. Opin. Struct. Biol. **44**, 18 (2017).

[3] A. K. Rai, J.-X. Chen, M. Selbach, and L. Pelkmans, Nature (London) **559**, 211 (2018).

[4] E. A. Marnik and D. L. Updike, Traffic **20**, 373 (2019).

[5] C. P. Brangwynne, C. R. Eckmann, D. S. Courson, A. Rybarska, C. Hoege, J. Gharakhani, F. Jülicher, and A. A. Hyman, Science **324**, 1729 (2009).

[6] C. P. Brangwynne, T. J. Mitchison, and A. A. Hyman, Proc. Natl. Acad. Sci. U.S.A. **108**, 4334 (2011).

[7] A. A. Hyman and K. Simons, Science **337**, 1047 (2012).

[8] C. F. Lee, C. P. Brangwynne, J. Gharakhani, A. A. Hyman, and F. Jülicher, Phys. Rev. Lett. **111**, 269902(E) (2013).

[9] A. A. Hyman, C. A. Weber, and F. Jülicher, Annu. Rev. Cell Dev. Biol. **30**, 39 (2014).

[10] S. Boeynaems, S. Alberti, N. L. Fawzi, T. Mittag, M. Polymenidou, F. Rousseau, J. Schymkowitz, J. Shorter, B. Wolozin, L. V. D. Bosch, P. Tompa, and M. Fuxreiter, Trends Cell Biol. **28**, 420 (2018).

[11] S. Alberti, A. Gladfelter, and T. Mittag, Cell **176**, 419 (2019).

[12] G. Franzese, G. Malescio, A. Skibinsky, S. V. Buldyrev, and H. E. Stanley, Nature (London) **409**, 692 (2001).

[13] Y. Katayama, T. Mizutani, W. Utsumi, O. Shimomura, M. Yamakata, and K.-I. Funakoshi, Nature (London) **403**, 170 (2000).

[14] H. Tanaka, Phys. Rev. E **62**, 6968 (2000).

[15] C. Huang, M. Olvera de la Cruz, and B. Swift, Macromolecules **28**, 7996 (1995).

[16] S. Mao, D. Kuldinow, M. P. Haataja, and A. Košmrlj, Soft Matter **15**, 1297 (2019).

[17] L. A. Amos and W. B. Amos, *Molecules of the Cytoskeleton* (Macmillan International Higher Education, London, 1991).

[18] J. Howard, *Mechanics of Motor Proteins and the Cytoskeleton* (Sinauer Assoc., Inc., Sunderland, MA, 2001).

[19] R. W. Style, T. Sai, N. Fanelli, M. Ijavi, K. Smith-Mannschott, Q. Xu, L. A. Wilen, and E. R. Dufresne, Phys. Rev. X **8**, 011028 (2018).

[20] K. A. Rosowski, T. Sai, E. Vidal-Henriquez, D. Zwicker, R. W. Style, and E. R. Dufresne, Nat. Phys. **16**, 422 (2020).

[21] J. Y. Kim, Z. Liu, B. M. Weon, T. Cohen, C.-Y. Hui, E. R. Dufresne, and R. W. Style, Sci. Adv. **6**, eaaz0418 (2020).

[22] K. A. Rosowski, E. Vidal-Henriquez, D. Zwicker, R. W. Style, and E. R. Dufresne, Soft Matter **16**, 5892 (2020).

[23] E. Vidal-Henriquez and D. Zwicker, Soft Matter **16**, 5898 (2020).

[24] M. Kothari and T. Cohen, J. Mech. Phys. Solids **145**, 104153 (2020).

[25] M. Doi, *Soft Matter Physics* (Oxford University Press, Oxford, 2013).

[26] J. Zhu, T. Li, S. Cai, and Z. Suo, J. Adhes. **87**, 466 (2011).

[27] S. B. Hutchens, S. Fakhouri, and A. J. Crosby, Soft Matter **12**, 2557 (2016).

[28] See Supplemental Material at http://link.aps.org/supplemental/10.1103/PhysRevLett.125.268001 for more details of theoretical derivations.

[29] P.-G. De Gennes, *Scaling Concepts in Polymer Physics* (Cornell University Press, Ithaca, 1979).

[30] A. N. Gent, Rubber Chem. Technol. **69**, 59 (1996).

[31] M. C. Boyce and E. M. Arruda, Rubber Chem. Technol. **73**, 504 (2000).

[32] A. N. Gent and D. A. Tompkins, J. Appl. Phys. **40**, 2520 (1969).

[33] A. N. Gent and C. Wang, J. Mater. Sci. **26**, 3392 (1991).

[34] M. B. Sweatman, R. Fartaria, and L. Lue, J. Chem. Phys. **140**, 124508 (2014).

[35] M. B. Sweatman and L. Lue, Adv. Theory Simul. **2**, 1900025 (2019).

[36] M. Decker, S. Jaensch, A. Pozniakovsky, A. Zinke, K. F. O'Connell, W. Zachariae, E. Myers, and A. A. Hyman, Curr. Biol. **21**, 1259 (2011).

[37] M. Rubinstein and R. H. Colby, *Polymer Physics* (Oxford University Press, Oxford, 2003).